Stellar binaries in galactic nuclei

Bradnick, B; Mandel, Ilya; Levin, Y.

DOI:
10.1093/mnras/stx1007

License:
Other (please specify with Rights Statement)

Document Version
Publisher's PDF, also known as Version of record

Citation for published version (Harvard):
Bradnick, B, Mandel, I & Levin, Y 2017, 'Stellar binaries in galactic nuclei: tidally stimulated mergers followed by tidal disruptions', *Royal Astronomical Society. Monthly Notices*, pp. 2042-2048.
https://doi.org/10.1093/mnras/stx1007

Monthly Notices of the ROYAL ASTRONOMICAL SOCIETY

MNRAS **469,** 2042–2048 (2017) doi:10.1093/mnras/stx1007
Advance Access publication 2017 April 26

Stellar binaries in galactic nuclei: tidally stimulated mergers followed by tidal disruptions

B. Bradnick,[1] I. Mandel[1,2]★ and Y. Levin[3]

[1]*School of Physics and Astronomy and Institute of Gravitational Wave Astronomy, University of Birmingham, Birmingham B15 2TT, United Kingdom*
[2]*Kavli Institute for Theoretical Physics, Santa Barbara, CA 93106, USA*
[3]*Monash Center for Astrophysics and School of Physics and Astronomy, Monash University, Clayton, VIC 3800, Australia*

Accepted 2017 April 21. Received 2017 April 21; in original form 2017 March 16

ABSTRACT

We investigate interactions of stellar binaries in galactic nuclear clusters with a massive black hole (MBH). We consider binaries on highly eccentric orbits around the MBH that change due to random gravitational interactions with other stars in the nuclear stellar cluster. The pericentres of the orbits perform a random walk, and we consider cases where this random walk slowly brings the binary to the Hills tidal separation radius (the so-called empty loss-cone regime). However, we find that in a majority of cases, the expected separation does not occur and instead the members of the binary merge together. This happens because the binary's eccentricity is excited by tidal interactions with the MBH, and the relative excursions of the internal eccentricity of the binary far exceed those in its internal semimajor axis. This frequently reduces the pericentre separation to values below typical stellar diameters, which induces a significant fraction of such binaries to merge ($\gtrsim$75 per cent in our set of numerical experiments). Stellar tides do not appreciably change the total rate of mergers but circularize binaries, leading to a significant fraction of low-eccentricity, low-impact-velocity mergers. Some of the stellar merger products will then be tidally disrupted by the MBH within $\sim 10^6$ yr. If the merger strongly enhances the magnetic field of the merger product, this process could explain observations of prompt relativistic jet formation in some tidal disruption events.

Key words: binaries: close – stars: kinematics and dynamics – galaxies: nuclei.

1 INTRODUCTION

Dozens of tidal disruption event (TDE) candidates have been observed at a variety of wavelengths, including X-rays (Komossa & Greiner 1999; Komossa et al. 2004; Burrows et al. 2011; Levan et al. 2011), UV (Gezari et al. 2009; Bloom et al. 2011), optical (van Velzen et al. 2011; Gezari et al. 2012; Arcavi et al. 2014; Chornock et al. 2014; Holoien et al. 2014) and radio (Zauderer et al. 2011). The physics of tidal disruptions, including the theoretical investigation of TDE light curves, have been explored by Rees (1988); Phinney (1989); Magorrian & Tremaine (1999); Lodato, King & Pringle (2009); Strubbe & Quataert (2009); MacLeod, Guillochon & Ramirez-Ruiz (2012); Guillochon & Ramirez-Ruiz (2013); Shen & Matzner (2014); Shiokawa et al. (2015); Bonnerot et al. (2016b) and others.

The majority of stars are members of stellar binaries. Binaries in a galactic nuclear cluster can scatter off other objects in the dense ($\gtrsim 10^6\,\mathrm{pc}^{-3}$) stellar cluster (Spitzer & Hart 1971; Antonini et al. 2010) surrounding the central massive black hole (MBH) on to highly eccentric orbits around the MBH. Tidal interactions with the MBH can then separate the binary; in the classical picture, one component may be ejected as a hypervelocity star (Hills 1988; Yu & Tremaine 2003; Gualandris, Portegies Zwart & Sipior 2005; Brown et al. 2005; Sari, Kobayashi & Rossi 2010; Brown 2015), while the other may be subsequently tidally disrupted by the MBH.

Mandel & Levin (2015) investigated binaries that were scattered towards the MBH from large radii. A single scattering event could move such binaries on to nearly radial orbits around the MBH, fully populating the loss cone around the MBH (Lightman & Shapiro 1977). The component stars of such binaries may be tidally disrupted directly following the tidal separation of the binary, leading to double TDEs; Mandel & Levin (2015) estimated that 5 to 10 per cent of all TDEs could be double TDEs. Only about 6 per cent of the simulated binaries in the full loss cone were brought to merger by tidal interactions with the MBH.

We complete the earlier work of Mandel & Levin (2015) by considering binaries that are scattered towards the MBH from smaller radii. The reduced lever arm means that such binaries cannot immediately transition on to nearly radial orbits, i.e. into the loss cone for tidal separation, but may instead gradually and stochastically approach the tidal-separation loss cone through small angular

★ E-mail: imandel@star.sr.bham.ac.uk

momentum changes over many orbits. Binaries on orbits that pass within a few tidal separation radii from the MBH experience tidal perturbations. These perturbations can significantly change the angular momentum of the inner binary without significantly modifying its energy. The eccentricity of the inner binary can be driven close to unity, resulting in a binary merger. In contrast to the low fraction of tidally stimulated mergers of binaries in the full loss cone, we find that 80 per cent of the empty loss cone binaries that we simulate result in high-eccentricity mergers, with the remainder becoming tidally separated.

When stellar tides between the binary components are introduced following an equilibrium tide model (Hut 1981), the merging fraction drops slightly to 75 per cent, with the remaining binaries being tidally separated. In the presence of stellar tides, about half of the binaries merge at high eccentricity as before, but the other half merge with low eccentricities ($e \lesssim 0.2$) due to efficient tidal circularization of the binary's inner orbit. As a result of stellar tides, these binaries merge at lower semimajor axes.

Mergers of binaries on less eccentric orbits around the MBH as a result of Lidov–Kozai (LK) resonances (Lidov 1962; Kozai 1962), and stellar evolution have been previously considered by Antonini et al. (2010); Prodan, Antonini & Perets (2015) and Stephan et al. (2016). In particular, Antonini et al. (2010) also investigated stellar binaries around an MBH with lower eccentricities than in this study, concluding that Lidov–Kozai (LK) oscillations played a dominant role in producing stellar mergers. However, as we show here, LK resonance is suppressed for binaries on highly eccentric orbits around the MBH because scattering relaxation interactions with the surrounding stellar cusp change the angular momentum of the binary's centre of mass around the MBH on a time-scale that is shorter than the LK time-scale. Moreover, merger products from lower eccentricity orbits are less likely to tidally interact with the MBH shortly after merger.

On the other hand, the merger products arising from binaries on very eccentric orbits around the MBH can be tidally disrupted by the MBH on time-scales of a million years or less. As well as being more massive and appearing rejuvenated, the merger products can have their magnetic fields strongly enhanced as a result of the merger (Wickramasinghe, Tout & Ferrario 2014; Zhu et al. 2015, however, Guillochon & McCourt 2017 and Bonnerot et al. 2016a criticized the Zhu et al. 2015 result, arguing that it did not incorporate a satisfactory magnetic field divergence cleaning scheme). Prompt jets have been observed in the Swift J164449.3+573451 TDE (Bloom et al. 2011; Burrows et al. 2011; Levan et al. 2011; Zauderer et al. 2011). Initial large-scale magnetic fields can aid in prompt jet production (Tchekhovskoy et al. 2014a), but may not be required (Parfrey, Giannios & Beloborodov 2015). Tidal disruptions of the products of recent tidally stimulated mergers with amplified magnetic fields may be potential candidates for prompt jet formation.

The structure of this paper is as follows. In section 2, we provide details of our binary population model, integration methods, the evolution of the angular momentum of the orbit around the MBH and the stellar tides model. We present our results in section 3. We discuss the implications of the results and the limitations of this work in section 4.

2 METHODS

We numerically integrate the trajectories of 1000 individual stellar binaries on highly eccentric orbits around an MBH, following an approach similar to Gould & Quillen (2003). We model the very eccentric orbit around the MBH as a parabolic orbit and numerically integrate only the near-periapsis portion of the orbit, over ∼20 inner orbital periods, where tidal effects from the MBH on the inner binary are greatest. We make use of the *IAS15* integrator in the REBOUND software package (Rein & Liu 2012; Rein & Spiegel 2015, see acknowledgments for more details).

In between the integrated periapsis passages, the orbit around the MBH evolves due to two-body relaxation. Each system is evolved until the stellar binary is either tidally separated or undergoes a merger, defined as the stars approaching to a separation smaller than the sum of their radii.

We evaluate the impact of stellar tides by integrating the same set of 1000 simulations with a simple prescription for equilibrium tides adapted from Eggleton & Kiseleva-Eggleton (2001). The following subsections contain details of the population model.

2.1 Binary population

We use the same approach as Mandel & Levin (2015) to generate the stellar binary properties. The mass M_1 of the primary star is generated from the Kroupa initial mass function (Kroupa 2001), in the range $M_1 \in [0.1, 100]\,\mathrm{M}_\odot$. The mass of the secondary is drawn according to the mass ratio $q = M_2/M_1$ distribution $p(q) \propto q^{-3/4}$, $q \in [0.2, 1.0]$, consistent with observations (Duquennoy & Mayor 1991; Reggiani & Meyer 2011; Sana et al. 2013). The radius of each main-sequence star is set using the approximate relationship $R_* = (M_*/\mathrm{M}_\odot)^k\,\mathrm{R}_\odot$ (Kippenhahn & Weigert 1994), with $k = 0.8$ for $M_* < \mathrm{M}_\odot$ and $k = 0.6$ when $M_* \geq \mathrm{M}_\odot$.

The semimajor axis a of the stellar binary is randomly drawn from $p(a) \propto 1/a$ (Öpik 1924) with an upper limit of 1 au and a lower limit set by the requirement that both stars must initially fit within their Roche lobes at periapsis (Eggleton 1983). The binary is further constrained to lie in the range of orbital periods $P_{\rm bin} \in [0.1\,\mathrm{d}, 1\,\mathrm{yr}]$. The upper limits in these constraints ensure that the binary is sufficiently compact to avoid disruption through interactions with other stars in the nuclear cluster.

The initial eccentricity distribution is based on Duquennoy & Mayor (1991), and is determined from the inner orbital period. Binaries with short periods (under 10 d) are placed on circular orbits and the remaining binaries have their eccentricities e drawn from a Gaussian with mean $\mu = 0.3$ and standard deviation $\sigma = 0.15$. The orbital plane of the inner (binary) orbit is randomly orientated with respect to the outer orbital plane (around the MBH), with the mutual inclination drawn uniformly in $\cos i \in [-1, 1]$ and the argument of periapsis and longitude of ascending node uniformly drawn from $\omega, \Omega \in [0, 2\pi]$.

2.2 Outer orbit around the MBH

We consider binaries that have been scattered on to high eccentricity orbits around the MBH of mass $M_{\rm MBH} = 10^6\,\mathrm{M}_\odot$. The angular momentum of the binary's orbit around the MBH will wander due to interactions with stars in the Bahcall–Wolf cusp. This cusp, with number density $n(r) \propto r^{-7/4}$, contains $N \sim 10^6$ stars in the MBH sphere of influence extending out to ∼1 pc (Merritt 2004).

Mandel & Levin (2015) explored binaries in the full loss cone for which the typical change $\langle \mathrm{d}h \rangle$ in angular momentum during one orbit around the MBH was larger than the minimum angular momentum for tidal disruption by the MBH (Lightman & Shapiro 1977):

$$h_{\rm LC} \sim \sqrt{G M_{\rm MBH} a \left(\frac{M_{\rm MBH}}{M_{\rm bin}}\right)^{1/3}}. \quad (1)$$

In this work, we instead focus on binaries that live in the empty loss cone and slowly explore the angular momentum space. This allows the MBH to gradually tidally perturb the inner orbit over many orbital passages near the MBH. The typical fractional evolution of the angular momentum per orbit for our population of binaries is $\langle \mathrm{d}h \rangle / h_{\mathrm{LC}} \sim 0.1$.

The time-scale for two-body relaxation to change the angular momentum by that of a circular orbit ($h_{\mathrm{circ}} = \sqrt{GMr}$) is given by Spitzer & Hart (1971):

$$\tau_{\mathrm{relax}} = \frac{v^3}{15.4 G^2 n m_*^2 \log \Lambda}, \tag{2}$$

where $m_* \sim 0.5\,\mathrm{M}_\odot$ is the typical stellar mass, n is the local stellar density, $v \sim \sqrt{GM_{\mathrm{MBH}}/r}$ is the typical stellar velocity at distance r from the MBH and $\Lambda \sim 0.4N$ is the Coulomb logarithm. The typical change in the angular momentum during one orbit is given by

$$\langle \mathrm{d}h \rangle = h_{\mathrm{circ}} \left[\frac{P_{\mathrm{out}}}{\tau_{\mathrm{relax}}} \right]^{1/2}, \tag{3}$$

where P_{out} is the outer orbital period. We model this angular momentum evolution as a random walk, applying a single isotropically oriented kick to the outer orbit once per passage around the MBH. Each directional component of this 3D kick is drawn from $\Delta h_i = \mathcal{N}(0, (\langle \mathrm{d}h \rangle / \sqrt{3})^2)$.

We randomly generate an entire trajectory of up to 1000 kicks prior to commencing the integration of a given binary. We start our simulation when the initial periapsis of the outer orbit is five times the tidal separation radius of the binary, defined as $r_{\mathrm{p,out}} = 5R_{\mathrm{TS}} \approx 5a(M_{\mathrm{MBH}}/M_{\mathrm{bin}})^{1/3}$ (Miller et al. 2005), where R_{TS} is the tidal separation radius of the binary and $M_{\mathrm{bin}} = M_1 + M_2$ is the mass of the binary. The apoapsis distance is drawn to be consistent with the Bahcall–Wolf cusp with $n(r) \propto r^{-7/4}$, within the range $r_{\mathrm{a,out}} \in [100 r_{\mathrm{p,out}}, 1\,\mathrm{pc}]$. This yields a semimajor axis of $a_{\mathrm{out}} = (r_{\mathrm{p,out}} + r_{\mathrm{a,out}})/2$ and a minimum initial eccentricity of $e_{\mathrm{out}} > 0.98$. A kick trajectory is accepted if it results in the periapsis of the outer orbit reaching the tidal disruption radius of the binary's hypothetical merger product.

2.3 Stellar tides

Many of our simulated binaries are on close orbits where stellar tides can efficiently circularize the orbit. We implement a simple equilibrium tide model (Hut 1981) between the inner binary stars, using equations formulated in Eggleton & Kiseleva-Eggleton (2001). We consider only the quadrupolar distortion of each star due to its inner binary companion, and ignore additional effects from stellar rotation. The periapsis of the inner binary is held constant while the eccentricity evolution follows

$$\frac{1}{e}\frac{\mathrm{d}e}{\mathrm{d}t} = -V_1 - V_2, \tag{4}$$

where the component V_i for star i in the inner binary is calculated as

$$V_i = \frac{9}{\tau_{\mathrm{TF},i}} \left[\frac{1 + (15/4)e^2 + (15/8)e^4 + (5/64)e^6}{(1-e^2)^{13/2}} \right], \tag{5}$$

where $\tau_{\mathrm{TF,\,i}}$ is the tidal friction time-scale. This time-scale depends on the viscous time-scale $\tau_{\mathrm{v,\,i}}$ and can be calculated using the expression (Eggleton & Kiseleva-Eggleton 2001)

$$\tau_{\mathrm{TF},i} = \frac{\tau_{\mathrm{v},i}}{9} \left(\frac{a}{R_i} \right)^8 \frac{M_i^2}{M_{\mathrm{bin}} M_j} (1 - Q_i)^2, \tag{6}$$

Table 1. Parameters used in the mass–luminosity relationship to obtain the approximate luminosity for a range of stellar masses (Duric 2012, Salaris & Cassisi 2005).

Mass ($\mathrm{M}_\odot$)	α	β
<0.43	0.23	2.3
0.43–2.00	1.00	4.0
2.00–20.00	1.50	3.5
20.00 <	2700.00	1.0

Table 2. A comparison of relevant time-scales relating to the binary. P_{bin} is the binary orbital period. The eccentricity evolution time-scale is the median value for a given eccentricity.

Time-scale	Length (yr)	Scaling
P_{bin}	$\sim 10^{-2}$	$\propto a^{3/2} M_{\mathrm{bin}}^{-1/2}$
τ_{v}	$\sim 10^{2}$	$\propto M^{(1-\beta)/3} R^{2/3} \alpha^{-1}$
P_{out}	$\sim 10^{4}$	$\propto a_{\mathrm{out}}^{3/2} M_{\mathrm{MBH}}^{-1/2}$
τ_{LK}	$\sim 10^{5}$	$\propto P_{\mathrm{out}}^2 P_{\mathrm{bin}}^{-1} (1 - e_{\mathrm{out}}^2)^{3/2}$
τ_{relax}	$\sim 10^{9}$	$\propto M_{\mathrm{MBH}}^{3/2} a_{\mathrm{out}}^{-3/2} n^{-1} m_*^2 \log 0.4N$
$\tau_{e=0.5}$	$\sim 10^{7}$	See section 2.3
$\tau_{e=0.9}$	$\sim 10^{3}$	”

where M_j is the mass of the binary companion. The term Q describes the quadrupole deformability of the star, and we adopt a value consistent with an $n = 3$ polytrope star, $Q = 0.021$ (calculated from the interpolation formula provided in Eggleton, Kiseleva & Hut 1998). An estimate of the viscous time-scale can be obtained based on the convective turnover time-scale (Zahn 1977) and includes a factor from integrating the square of the rate-of-strain tensor of the time-dependent velocity field over the star (Eggleton & Kiseleva-Eggleton 2001), γ_i:

$$\tau_{\mathrm{v},i} = \frac{1}{\gamma_i} \left(\frac{3 M_i R_i^2}{L_i} \right)^{1/3}. \tag{7}$$

We set the value $\gamma_i = 0.01$ as in Eggleton & Kiseleva-Eggleton (2001), and the luminosity of the star, L, is determined from the mass–luminosity relationship $L/\mathrm{L}_\odot = \alpha (M/\mathrm{M}_\odot)^\beta$, with the parameters α and β provided in Table 1.

As listed in Table 2, the tidal evolution time-scale is much greater than the periapsis passage time-scale for our binaries. Therefore, we only include tidal evolution by adjusting the binary parameters between periapsis passages around the MBH. We calculate the median tidal evolution time-scale $\tau_{\mathrm{e}} = e/(\mathrm{d}e/\mathrm{d}t)$ at two different fiducial values of the eccentricity to show the strong dependence on eccentricity. This time-scale is longer than the $\sim 10^4$-yr outer orbital period for the majority of our binaries until the inner eccentricity reaches $e \sim 0.8$; above this value stellar tides become efficient in circularizing half of the population over the course of an outer orbital period. We perform this tidal evolution using a fourth-order Runge–Kutta–Cash–Karp method.

3 RESULTS OF NUMERICAL INTEGRATIONS

The internal angular momentum of stellar binaries gradually approaching the boundary of the loss cone around the MBH typically walks much more than their internal energy. Gradual tidal

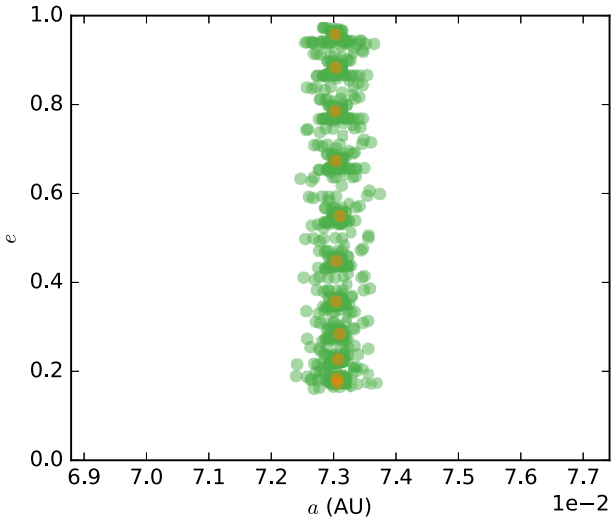

Figure 1. Typical evolution of a stellar binary gradually approaching the empty loss cone. The eccentricity is able to grow from an initially small value $e \sim 0.2$ to $\gtrsim 0.95$, whilst the semimajor axis only varies slightly. Orange points mark the initial parameters of the inner binary for each orbit around the MBH, and the green points show the fluctuations during the near-periapsis passages.

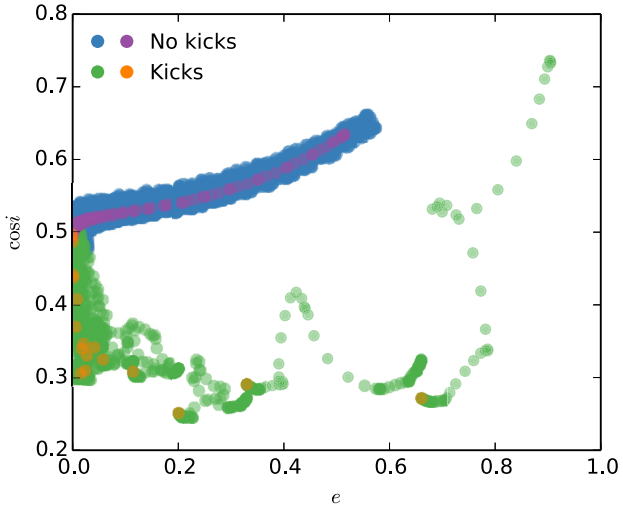

Figure 2. The evolution of the inner orbit of a typical stellar binary, showing the eccentricity and cosine of inclination over multiple trajectories around the MBH. Evolution is shown both with and without the angular momentum kicks to the outer orbit due to two-body relaxation. The primary colours show the elements throughout each trajectory around the MBH, whereas the secondary colours show the initial value for each periapsis passage.

interactions between the stellar binary and the MBH cause only relatively small fluctuations in the inner binary's energy:

$$\frac{\delta E}{E} \sim \frac{\delta a}{a} \sim \frac{M_{\rm BH}}{m_{\rm bin}} \frac{a^3}{r_{\rm p,out}^3} \sim \left(\frac{R_{\rm TS}}{r_{\rm p,out}} \right)^3 . \tag{8}$$

On the other hand, the eccentricity of the inner binary is able to evolve efficiently through tidal torques. Fig. 1 illustrates the typical evolution of a stellar binary; the eccentricity can be seen to grow from an initially small value of $e \sim 0.2$ to $\gtrsim 0.95$, while the semimajor axis stays constant to within ± 1 per cent.

These eccentricity fluctuations do not represent classical LK resonances. The LK time-scale for $M_{\rm bin} \ll M_{\rm MBH}$ and $1 - e_{\rm out} \ll 1$ is (Antognini 2015)

$$\tau_{\rm LK} \approx \frac{8}{15\pi} \frac{P_{\rm out}^2}{P_{\rm bin}} \left(1 - e_{\rm out}^2\right)^{3/2} \approx 0.5 \frac{r_{\rm p,out}^{3/2}}{r_{\rm TS}^{3/2}} \frac{P_{\rm out}^2}{P_{\rm bin}} . \tag{9}$$

Substituting in the initial periapsis of the systems we are investigating $r_{\rm p,out} = 5 r_{\rm TS}$ yields a LK time-scale that is approximately five times the orbital period around the MBH (cf. Table 2). Therefore the angular momentum kicks that the binary's orbit around the MBH receives at apoapsis due to two-body relaxation destroy the coherence required for LK resonance and suppress classical LK oscillations.

This suppression is demonstrated in Fig. 2, where we compare the evolution of two otherwise identical systems, with and without angular momentum kicks applied far from the MBH. Without these kicks, the evolution is coherent and can be seen to follow LK-like behaviour where the projection of the angular momentum of the binary on to the orbital angular momentum axis remains almost constant. When these kicks are included, the evolution of the inner orbital parameters appears chaotic and can reach very high eccentricities in tens of orbits around the MBH.

Such eccentricity excursions lead to a high fraction of tidally stimulated mergers. The vast majority of the simulated binaries, just under 80 per cent, result in mergers. As expected, mergers typically happen at the highest eccentricities, when the inter-star separation at periapsis decreases. Although ∼85 per cent of the stellar binaries we simulated are initially circular, the final distribution is 'super-thermal' (steeper than $p(e) = 2e$), as shown in Fig. 3. The merger fraction is highest for initially close binaries, which require smaller eccentricity excursions for merger (see Fig. 4). The remaining binaries are tidally separated, with one of the stars ejected as a hypervelocity star.

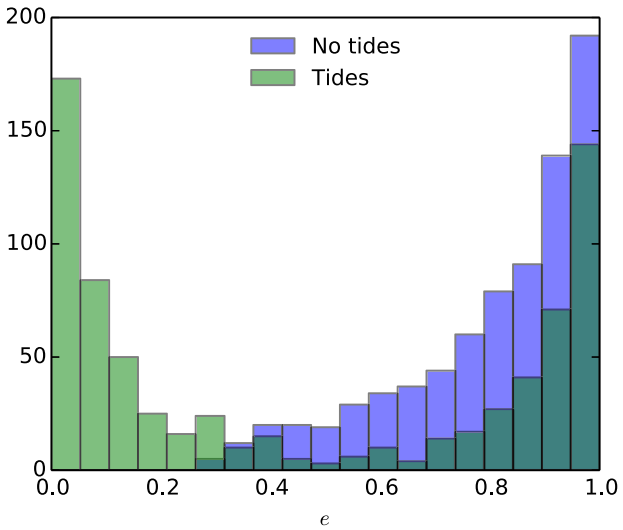

Figure 3. Final eccentricity distribution of merging systems both with and without tides acting between the inner binary components.

The inclusion of stellar tides slightly decreases the overall fraction of mergers to ∼75 per cent as high-eccentricity excursions are partially suppressed by tides. Fig. 3 shows a bimodal distribution of inner binary eccentricities once tides are included, with many binaries circularized by tides. While tides circularize these binaries, they also harden them; this ensures that merger rather than tidal separation remains the most likely evolutionary outcome. The dependence of the merger fraction on initial separation with stellar tides remains similar to Fig. 4 and is not included here.

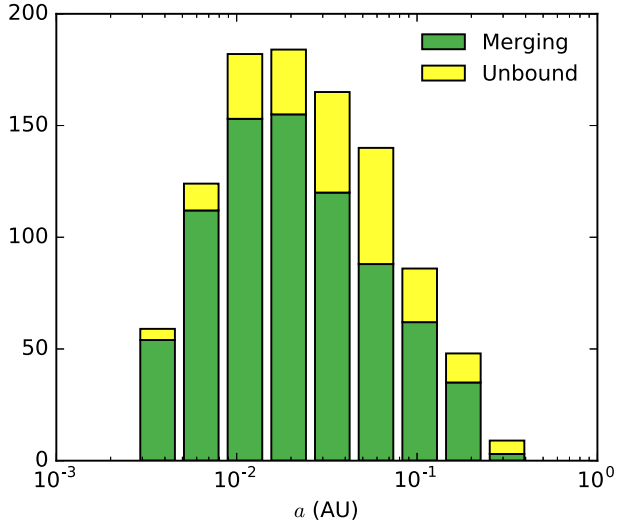

Figure 4. Initial binary semimajor axes categorized by the binary's fate (no stellar tides).

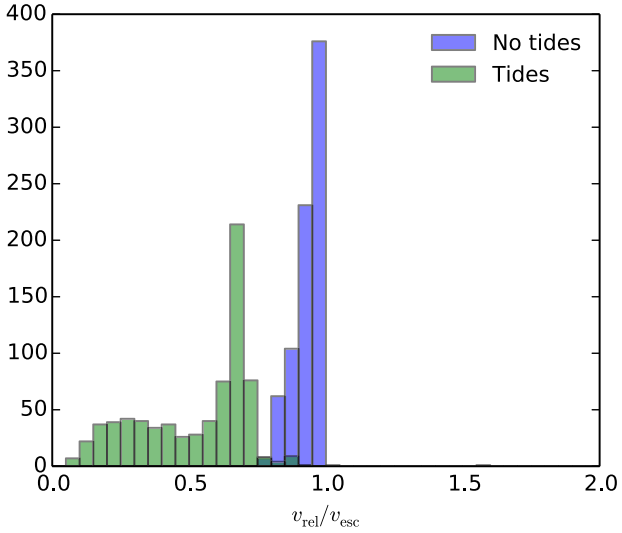

Figure 5. Relative velocity at point of impact for merging systems in units of the escape velocity of the primary star, with and without stellar tides.

The circularizing impact of stellar tides significantly changes the collision dynamics when the merger happens. The relative velocities between colliding stars are shown in Fig. 5. Collisions in the absence of stellar tides, which typically happen at a high impact velocity, reaching the escape velocity at the surface of the more massive star, are likely to lead to significant mass loss and an extended merger product. Meanwhile, grazing collisions in the tidally circularized binaries can have significantly lower relative velocities.

Among the simulated population of binaries most still require ∼100 orbits after merger before the merger product is disrupted. Fig. 6 shows the distribution of the time between the tidally stimulated merger and the tidal disruption of the merger product, under the assumption that the merger itself does not alter the trajectory around the MBH. Merger products can be disrupted in as little as $\sim 10^5$ yr. The inclusion of stellar tides does not appreciably change this distribution.

Although mergers are more common than binary tidal separations in our simulations, a considerable number of hypervelocity stars (HVS) are still produced. The distribution of hyperbolic excess

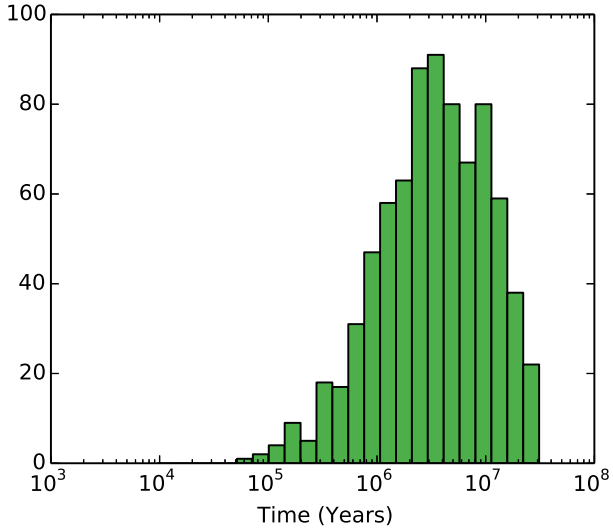

Figure 6. Time delay distribution between the tidally stimulated mergers and the tidal disruption of the merger product by the MBH in our simulations, chosen so that the merger product would approach to within its tidal disruption periapsis of the MBH within 1000 outer orbits. A tail of longer time delays is omitted through this choice; see Section 4.

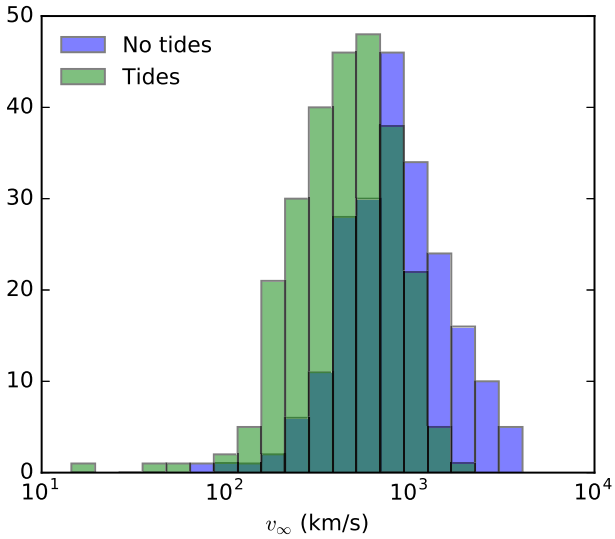

Figure 7. The distribution of hyperbolic excess velocities of tidally ejected stars.

velocities of the ejected stars in tidally separated binaries $v_\infty^2 = v_*^2 - 2GM_{\rm MBH}/r$, where v_* is the star's current velocity and r is the radial distance from the star to the MBH, is shown in Fig. 7. A number of stars are ejected with velocities exceeding 1000 km s^{-1}. Stellar tides generally reduce ejection velocities.

4 DISCUSSION

We simulated the dynamics of stellar binaries in the empty loss cone around an MBH. These systems preferentially merge over becoming tidally separated as the tide on the binary from the MBH efficiently drives eccentricity evolution without significantly affecting the binary's energy (see Fig. 1). We found that stellar binaries on highly eccentric orbits that gradually diffuse in angular momentum produce mergers in $\gtrsim$75 per cent of our simulations. The remaining binaries become tidally separated and produce HVS with hyperbolic

excess velocities up to 1000 km s^{-1}. Consequently, more than ten percent of all TDEs should be disruptions of merger products.

Such mergers may generate strong magnetic fields through a dynamo mechanism (Wickramasinghe et al. 2014). When the merger products are subsequently tidally disrupted by the MBH, these strong magnetic fields could play a crucial role in powering the prompt formation of jets such as observed in Swift J164449.3+573451 (Giannios & Metzger 2011).

Stellar tides between the binary components slightly reduce the merging fraction, and significantly reduce the eccentricity of the binary at the time of merger for many systems, thereby reducing the collision velocity. We used an equilibrium tide model that only includes quadrupolar terms in the stellar deformation and loses accuracy at high eccentricity. A more careful treatment of tides would include a dynamical tide model (e.g. Fabian, Pringle & Rees 1975; Press & Teukolsky 1977; Zahn 1977) and additional effects from stellar rotation and tides raised by the MBH. This would increase tidal efficiency for very eccentric systems, possibly further reducing the eccentricity and relative velocity at merger.

The treatment of the collision could be improved with more detailed hydrodynamical simulations to more accurately determine the structure of the merger product (Antonini, Lombardi & Merritt 2011), the mass loss from the system and any change in the trajectory of the merger product following merger, which we have ignored in our simplified analysis. Moreover, Roche lobe overflow as the stars approach prior to merger could lead to a softer collision.

Stephan et al. (2016) found that stellar evolution played an important role in the evolution of 65 per cent of the binaries they simulated in orbit around an MBH. However, stellar evolution is unlikely to significantly affect our results, as these systems evolve on a typical time-scale of ∼Myr.

We assumed a Bahcall–Wolf cusp around the MBH. The stellar density affects the efficiency of two-body relaxation at a given radius (see equation 2); therefore, a different stellar density profile would shift the boundary between the empty loss cone and the full loss cone. However, the behaviour of binaries within the empty loss cone for tidal separation will not be significantly affected, and ∼50 per cent of tidally impacted binaries would still come from the empty loss cone regime.

We populated stellar binaries according to the observed mass, period and eccentricity distributions (see Section 2.1). If tighter/wider orbits are favoured, the fraction of tidally induced mergers would increase/decrease, as indicated by the anti-correlation between the orbital separation and merger fraction in Fig. 4. Meanwhile, the component mass is not significantly correlated with the fate of the binary; therefore, varying the mass distribution should not appreciably impact the merger fraction. The vast majority of the relatively short-period binaries analysed here are expected to be tidally circularized, with negligible initial eccentricities.

The shortest period binaries with the highest orbital velocity are expected to produce the fastest HVS when the binary is tidally separated by an MBH. However, our simulations show that the closest binaries are preferentially merged rather than tidally separated in the empty loss cone. This depletes the high-velocity tail of the hypervelocity star distribution, especially when stellar tides are included. The absence of the high-velocity tail appears consistent with observations of Galactic HVS (Rossi, Kobayashi & Sari 2014; Rossi et al. 2017). However, the tidally stimulated merger fraction is significantly lower for binaries in the full loss cone (Mandel & Levin 2015), so full loss cone binaries could still provide contributions to the high-velocity tail unless other effects suppress tidal separations of close binaries in that regime.

Our simulations were selected to focus on binaries whose angular momentum random walk around the MBH will bring the merger product to a sufficiently small periapsis for tidal disruption within 1000 orbits. The actual fraction of merger products disrupted within a few million years is $\lesssim$10 per cent. A long delay could allow the merger product to return to equilibrium, reducing the stellar radius, but an enhanced magnetic field could be retained in the radiative zones of the merger product (Braithwaite & Spruit 2004). Moreover, many merger products will come sufficiently close to the MBH for partial disruption long before full tidal disruption, and the extended merger products will be particularly susceptible to partial disruptions. Guillochon & McCourt (2017) argue that such disruptions can increase the magnetic field by factors of ∼20. The combined effect of a merger followed by repeated partial disruptions can have a truly dramatic effect on the star's magnetic field. Tchekhovskoy et al. (2014b) argued that strong coherent fields are required for prompt jet formation. Parfrey et al. (2015) advocate a less stringent requirement for the large-scale field and the ability of small-scale fields to produce jets when interacting with a spinning black hole. Clearly, strong initial fields prior to disc formation can enhance the magnetic activity of the disc and jet formation. Tidally stimulated stellar mergers could thus be an important ingredient in the production of jets during subsequent TDEs.

ACKNOWLEDGEMENTS

Simulations in this paper made use of the IAS15 *N*-body integrator (Rein & Spiegel 2015) found in the REBOUND package (Rein & Liu 2012), which can be downloaded at http://github.com/hannorein/rebound. We are grateful to Will Farr, James Guillochon, Elena Maria Rossi and Alison Farmer for useful discussions. IM acknowledges partial support by the STFC and by the National Science Foundation under Grant No. NSF PHY11-25915. YL acknowledges research support by the Australian Research Council Future Fellowship.

REFERENCES

Antognini J. M. O., 2015, MNRAS, 452, 3610
Antonini F., Faber J., Gualandris A., Merritt D., 2010, ApJ, 713, 90
Antonini F., Lombardi Jr J. C., Merritt D., 2011, ApJ, 731, 128
Arcavi I. et al., 2014, ApJ, 793, 38
Bloom J. S. et al., 2011, Science, 333, 203
Bonnerot C., Price D. J., Lodato G., Rossi E. M., 2016a, MNRAS, preprint (arXiv:1611.09853)
Bonnerot C., Rossi E. M., Lodato G., Price D. J., 2016b, MNRAS, 455, 2253
Braithwaite J., Spruit H. C., 2004, Nature, 431, 819
Brown W. R., 2015, ARA&A, 53, 15
Brown W. R., Geller M. J., Kenyon S. J., Kurtz M. J., 2005, ApJ, 622, L33
Burrows D. N. et al., 2011, Nature, 476, 421
Chornock R. et al., 2014, ApJ, 780, 44
Duquennoy A., Mayor M., 1991, A&A, 248, 485
Duric N., 2012, Advanced Astrophysics. Cambridge Univ. Press, Cambridge
Eggleton P. P., 1983, ApJ, 268, 368
Eggleton P. P., Kiseleva-Eggleton L., 2001, ApJ, 562, 1012
Eggleton P. P., Kiseleva L. G., Hut P., 1998, ApJ, 499, 853
Fabian A. C., Pringle J. E., Rees M. J., 1975, MNRAS, 172, 15p
Gezari S. et al., 2009, ApJ, 698, 1367
Gezari S. et al., 2012, Nature, 485, 217
Giannios D., Metzger B. D., 2011, MNRAS, 416, 2102
Gould A., Quillen A. C., 2003, ApJ, 592, 935
Gualandris A., Portegies Zwart S., Sipior M. S., 2005, MNRAS, 363, 223
Guillochon J., McCourt M., 2017, ApJ, 834, L19

Guillochon J., Ramirez-Ruiz E., 2013, ApJ, 767, 25
Hills J. G., 1988, Nature, 331, 687
Holoien T. W.-S. et al., 2014, MNRAS, 445, 3263
Hut P., 1981, A&A, 99, 126
Kippenhahn R., Weigert A., 1994, Stellar Structure and Evolution. Springer-Verlag, p. 468
Komossa S., Greiner J., 1999, A&A, 349, L45
Komossa S., Halpern J., Schartel N., Hasinger G., Santos-Lleo M., Predehl P., 2004, ApJ, 603, L17
Kozai Y., 1962, AJ, 67, 591
Kroupa P., 2001, MNRAS, 322, 231
Levan A. J. et al., 2011, Science, 333, 199
Lidov M. L., 1962, Planet. Space Sci., 9, 719
Lightman A. P., Shapiro S. L., 1977, ApJ, 211, 244
Lodato G., King A. R., Pringle J. E., 2009, MNRAS, 392, 332
MacLeod M., Guillochon J., Ramirez-Ruiz E., 2012, ApJ, 757, 134
Magorrian J., Tremaine S., 1999, MNRAS, 309, 447
Mandel I., Levin Y., 2015, ApJ, 805, L4
Merritt D., 2004, in Ho L. C., ed, Coevolution of Black Holes and Galaxies, Cambridge Univ. Press, Cambridge, p. 263
Miller M. C., Freitag M., Hamilton D. P., Lauburg V. M., 2005, ApJ, 631, L117
Öpik E., 1924, Publ. Tartu Astrofizica Obs., 25
Parfrey K., Giannios D., Beloborodov A. M., 2015, MNRAS, 446, L61
Phinney E. S., 1989, in Morris M., ed., Proc. IAU Symp. 136, The Center of the Galaxy. Kluwer, Dordrecht, p. 543
Press W. H., Teukolsky S. A., 1977, ApJ, 213, 183
Prodan S., Antonini F., Perets H. B., 2015, ApJ, 799, 118
Rees M. J., 1988, Nature, 333, 523
Reggiani M. M., Meyer M. R., 2011, ApJ, 738, 60
Rein H., Liu S.-F., 2012, A&A, 537, A128
Rein H., Spiegel D. S., 2015, MNRAS, 446, 1424
Rossi E. M., Kobayashi S., Sari R., 2014, ApJ, 795, 125
Rossi E. M., Marchetti T., Cacciato M., Kuiack M., Sari R., 2017, MNRAS, 467, 1844
Salaris M., Cassisi S., 2005, Evolution of Stars and Stellar Populations. John Wiley & Sons
Sana H. et al., 2013, A&A, 550, A107
Sari R., Kobayashi S., Rossi E. M., 2010, ApJ, 708, 605
Shen R.-F., Matzner C. D., 2014, ApJ, 784, 87
Shiokawa H., Krolik J. H., Cheng R. M., Piran T., Noble S. C., 2015, ApJ, 804, 85
Spitzer Jr L., Hart M. H., 1971, ApJ, 164, 399
Stephan A. P., Naoz S., Ghez A. M., Witzel G., Sitarski B. N., Do T., Kocsis B., 2016, MNRAS, 460, 3494
Strubbe L. E., Quataert E., 2009, MNRAS, 400, 2070
Tchekhovskoy A., Metzger B. D., Giannios D., Kelley L. Z., 2014a, MNRAS, 437, 2744
Tchekhovskoy A., Metzger B. D., Giannios D., Kelley L. Z., 2014b, MNRAS, 437, 2744
van Velzen S. et al., 2011, ApJ, 741, 73
Wickramasinghe D. T., Tout C. A., Ferrario L., 2014, MNRAS, 437, 675
Yu Q., Tremaine S., 2003, ApJ, 599, 1129
Zahn J.-P., 1977, A&A, 57, 383
Zauderer B. A. et al., 2011, Nature, 476, 425
Zhu C., Pakmor R., van Kerkwijk M. H., Chang P., 2015, ApJ, 806, L1

This paper has been typeset from a TEX/LATEX file prepared by the author.